Fuel 268 (2020) 117363

Contents lists available at ScienceDirect

Fuel

journal homepage: www.elsevier.com/locate/fuel

Hydrotreating atmospheric gasoil and co-processing with rapeseed oil using supported Ni-Mo and Co-Mo carbide catalysts

Héctor De Paz Carmona*, Uliana Akhmetzyanova, Zdeněk Tišler, Pavla Vondrová

Unipetrol Centre for Research and Education, Block 2838, 436 70 Litvínov-Záluží 1, Czechia

A B S T R A C T

Sulfur-free Mo carbide catalysts supported on Al_2O_3 and TiO_2 have shown good activity during the co-processing of middle distillates with vegetable oils in prior studies. However, their hydrotreating activity is low compared with that of conventional hydrotreating catalysts. To increase the hydrotreating effectiveness, promoter metals, such as Ni or Co, can be added. This paper describes an extensive study on the use of four sulfur-free Ni-Mo and Co-Mo carbide catalysts (supported on Al_2O_3 and TiO_2) for the hydrotreatment of atmospheric gasoil (AGO) and co-processing with rapeseed oil (RSO). The tests were conducted in a fixed bed reactor unit at 330–350 °C, 5.5 MPa, a weigh hourly space velocity (WHSV) = 1–2 h^{-1}, and AGO/RSO of 100/0, 95/5, 90/10, and 75/25 wt.%. Analogous to conventional hydrotreatment catalysts, adding the promotor metals significantly increased the product quality and the hydrodesulfurisation and hydrodenitrogenation efficiencies at higher temperatures or at lower WHSVs. In the case of RSO co-processing, all the tested catalysts promoted the hydrodeoxygenation pathway instead of (hydro) decarboxylation/decarbonylation with an insignificant decrease in the hydrodesulfurization efficiency at lower AGO/RSO ratios. Therefore, our results suggest that promoting Mo carbide catalysts with Ni or Co significantly improves their catalytic properties, making them more competitive with conventional hydrotreating catalysts.

1. Introduction

The European Union Directive 2018/2001 established a binding union target to use at least 32% renewable energy by 2030, which means 12% more than in 2020. This supports and promotes the development of modern, more efficient, and eco-friendly biofuels to replace petroleum-based fuels, such as diesel and gasoline. Among the biofuels, FAME (fatty acid methyl ester), which is obtained by triglyceride transesterification, is probably one of the most known [1,2]. However, the hydrotreatment of vegetable oils is more advantageous due to the flexibility of the process. Thus, the possibility to co-process middle distillates with vegetable oils in existing hydrotreating units [3,4] makes the production of biofuels economically attractive.

Co-processing under common hydrotreating industrial conditions (350 – 370 °C and 7.0 – 8.0 MPa) removes sulfur, nitrogen, and metals from the middle distillates [5] and provides for deoxygenation of triglycerides and free fatty acids from vegetable oils [6]. During deoxygenation, the triglyceride molecule is hydrogenated and cleaved, producing three carboxylic acids and one molecule of C_3H_8. Then, the process continues according to three different pathways [7]: (i) hydrodeoxygenation (HDO) – producing two molecules of H_2O and linear paraffins with an even number of carbon atoms (normally nC_{16} and nC_{18}); (ii) (hydro)decarboxylation (HDC) – obtaining one molecule of CO and linear paraffins with an odd number of carbons (normally nC_{15} and nC_{17}); and (iii) (hydro)decarbonylation (HDCn) –producing one molecule of CO, one molecule of H_2O, and paraffins with an odd number of carbons, similar to the HDC pathway. The ratios of linear paraffins of different lengths formed by HDO and HDC/HDCn is highly dependent on the catalyst selectivity, which is determined by the operating conditions and the specific catalyst used [8].

The most common catalysts used for the co-processing of middle distillates with vegetable oils are commercial hydrotreating catalysts (supported sulfide Co-Mo/Al_2O_3 and Ni-Mo/Al_2O_3) [9]. However, with a high content of vegetable oil, the hydrodesulfurization (HDS) efficiency can decrease owing to the leaching of sulfur from the catalyst surface, making it necessary to add sulfiding agents (such as CS_2 or dimethyl disulfide (DMDS)) to the triglyceride feedstock [10]. Thus, the optimal vegetable oil content for co-processing is 5–10 wt% [11]. This is a significant obstacle for the final implementation of co-processing on an industrial scale. Thus, obtaining an increase in the percentage of biomass without any risk is a long-term priority for the development of new catalysts.

Therefore, sulfur-free-supported Mo carbide catalysts (MoCx) could be considered as promising alternatives to conventional hydrotreatment catalysts based on their capacities to absorb/activate H_2 and transfer it to reactant molecules [12]. Some previous studies have described the

* Corresponding author.
E-mail addresses: hector.carmona@unicre.cz (H. De Paz Carmona), uliana.akhmetzyanova@unicre.cz (U. Akhmetzyanova), zdenek.tisler@unicre.cz (Z. Tišler), pavla.vondrova@unicre.cz (P. Vondrová).

https://doi.org/10.1016/j.fuel.2020.117363
Received 10 October 2019; Received in revised form 3 February 2020; Accepted 7 February 2020
Available online 15 February 2020
0016-2361/

Nomenclature

AGO	Atmospheric gasoil
AGOR_X	Mixtures of AGO and RSO, X = content of RSO (wt.%)
ASTM	American Society for Testing and Materials
BET	Brunauer–Emmett–Teller method
FAME	Fatty acid methyl ester
HDC	(Hydro)decarboxylation
HDCn	(Hydro)decarbonylation
HDN	Hydrodenitrogenation
HDO	Hydrodeoxygenation
HDS	Hydrodesulfurization
HVO	Hydrogenated vegetable oil
ICP-OES	Inductively coupled plasma optical emission spectroscopy
ID	Internal diameter (mm)
MoCx	Mo carbide catalysts
OD	Outer diameter (mm)
PDF	Powder Diffraction Files
RSO	Rapeseed oil
S_{BET}	BET surface areas (m^2/g)
sp	Support precursor metal
TCD	Thermal conductivity detector
TOS	Time on stream (h)
TPR	Temperature-programmed reduction
WHSV	Weigh hourly space velocity (h^{-1})

use of MoCx catalysts for the HDS of middle distillates [13,14] and for the hydrotreatment of triglycerides [15,16], suggesting suitable use of these catalysts for hydrotreatment.

In the case of co-processing of sulfur/nitrogen and oxygen compounds, MoCx catalysts have demonstrated their capacity in simultaneous HDS and HDO reactions [17,18]. However, for deep desulfurisation of middle distillates (sulfur content < 10 ppm) during co-processing, conventional sulfide hydrotreatment catalysts seem to be more efficient [19,20], which makes mandatory the improvement of MoCx catalysts activity. Thus, one easy method includes the addition of a promotor metal, such as Ni or Co, to the catalyst [21], increasing its activity significantly owing to the ensemble and ligand effects [22]. This promotor effect has been reported by B. Diaz et al. [23] and J. Guangzhou et al. [24] in the context of the hydrotreatment of thiophene and dibenzothiophene with Mo, Ni-Mo, and Co-Mo carbide and nitride catalysts, resulting in a significant improvement in the catalyst activity. To study the suitability of Ni-Mo and Co-Mo carbide catalysts on an industrial scale, detailed research on the co-processing of middle distillates and vegetable oil under industrial conditions is required.

In line with previous work [18], this paper describes an extensive and detailed study of four sulfur-free-supported (Al_2O_3 and TiO_2) bimetallic (Ni-Mo and Co-Mo) carbide catalysts during the hydrotreating of atmospheric gasoil (AGO) and during its co-processing with rapeseed oil (RSO – 5, 10, and 25 wt%) under industrial operating conditions (330–350 °C, 5.5 MPa, a weigh hourly space velocity (WHSV) of 1–2 h^{-1}) as plausible alternatives to conventional hydrotreating catalysts. The aim of this work was to study the properties of bimetallic carbide catalysts (Co-Mo and Ni-Mo) and the influence of the operating conditions and RSO addition on the product properties and hydrotreating effectiveness (as defined by the HDS, hydrodenitrogenation (HDN), and hydrogenation efficiencies).

2. Materials and methods

2.1. Catalysts and feeds

Four Ni/Co–Mo carbide catalysts (NiMoCx and CoMoCx) were synthesized by an incipient wetness impregnation over commercial Al_2O_3 (Sasol) and TiO_2 (Euro support manufacturing) supports. Then, the materials underwent temperature-programmed reduction (TPR) to prepare the corresponding carbide phases. The synthesis of Mo carbides has been extensively detailed in a previous study [25]. A similar procedure was used to prepare the bimetallic catalyst samples.

The hexamethylenetetramine molybdenum complex, which was synthesised according to the Afanasiev method [26], was dissolved in 25% NH_3 and mixed with Ni or Co nitrates (Merck) to produce the Ni-Mo and Co-Mo precursors. Then, the precursors were loaded onto Al_2O_3 or TiO_2 supports (particle sizes of 0.224–0.560 mm). The impregnated samples were dried at 200 °C for 14 h in an air atmosphere. The formation of the carbide phase or carburisation was achieved in a tubular quartz reactor with an internal diameter (ID) of 27 mm and a length of 100 cm. The heating of the reactor was conducted using a triple-zone electric oven regulated by a PID (proportional–integral–derivative) controller. A fritted quartz cuvette with the impregnated sample was placed in the middle of the reactor and underwent TPR in a flow of 20 vol% CH_4 in H_2. The thermal treatment started at 200 °C (under N_2 flow), reaching 700 °C (under CH_4 in a H_2 flow) at a heating rate of 10 °C/min. The catalyst sample was held at the synthesis temperature for 3 h. Then, the reactor was cooled to room temperature by a nitrogen flow for 30 min. Finally, the catalyst sample was passivated with 1 vol% O_2 in Ar for 2 h. Once the synthesis procedure completed, the catalyst was transported immediately to the experimental unit under N_2 atmosphere to prevent oxidation. The experimental set up details are described in Section 2.2 below.

Each fresh catalyst sample was characterised by analytical methods. The crystallographic structure was determined using X-ray diffraction (XRD; D8 Advance ECO/Bruker). The patterns were collected over the 2θ range from 5 to 70° and evaluated using Diffrac. Eva software V 4.1.1. The specific surface area (BET, Brunauer–Emmett–Teller) was determined via N_2 physisorption (Autosorb iQ/Quantachrome instruments). The pore size distribution was measured via Hg porosimetry (AutoPore IV 9510 mercury porosimeter/Micrometrics instrument). The composition of the catalyst samples was determined using inductively coupled plasma optical emission spectroscopy (ICP-OES; Agilent 725/Agilent Technologies, Inc.) and elemental analysis (FLASH 2000 Combustion CHNS/O Analysed/Thermo).

The middle distillate used during the co-processing was AGO, which was obtained from the industrial atmospheric distillation of a Russian export blend crude oil. This petroleum feedstock was supplied by a commercial refinery. The RSO used was a food-quality commercial vegetable oil (ARO). Three different ratios of AGO/RSO were used during co-processing: 95/5, 90/10, and 75/25 wt.%/wt.%. Feedstocks and their mixtures were characterised by the density at 20 °C (ASTM – American Society of Testing and Materials – D 4052), the refractive index at 20 °C (ASTM D 1218), the sulfur content (ASTM D 1552), nitrogen content (ASTM D 5291), elemental analysis of C–H (ISO 29541), bromine number (ASTM D 1492), acid number (ASTM D 664) and simulated distillation (Simdis – ASTM D 2887). A standard refinery gas was used as the H_2 source (98.5–99.5 vol% of H_2 and 0.5–1.5 vol% of CH_4) for the hydrotreatment.

2.2. Experimental set up and catalytic tests

Hydrotreating experiments were carried out in a bench-scale unit using a stainless steel reactor with an ID of 17 mm. A thermowell with an outer diameter (OD) of 5 mm was placed in the axis of the reactor to measure and control the internal temperature. Heating of the reactor was performed with a triple-zone electric heater with independent control for each reactor zone. The unit was equipped with low- and high-pressure product collectors and a Kämmer valve placed behind the

product collector to control the pressure. To avoid plugging of the product pipelines during co-processing, the output lines of the reactor were heating to 50 °C. The unit is in the experimental facility of the UniCRE (Unipetrol Centre of Research and Education), located in Litvínov-Záluží, Czech Republic. Fig. 1 shows a scheme of the bench-scale unit used.

Before each experiment, 8.0 g of catalyst (particle size of 0.224 – 0.560 mm) was divided into four parts (2.0 g each) and mixed with a fine carborundum (SiC – 0.1 mm) in ratios of 1:1, 1:2, 1:3, and 1:4 (vol:vol). The four parts of the catalyst bed were loaded into the reactor from 1:1 to 1:4 to gradually increase the catalyst concentration along the reactor and to maintain the reaction temperature profile in the isothermal regime. After the catalyst loading finished, the reactor was flushed with N_2 (600 NL/h) at 25 °C and 100 kPa for 2 h. Then, the gas was changed from N_2 to H_2. The reactor was pressurised to 5.5 MPa at a H_2 flow of 50 NL/h and heated to 450 °C at a heating rate of 20 °C/h. After 4 h under these conditions, the reactor temperature was decreased to the initial working temperature (330 °C), and the H_2 flow was adjusted to correspond to 16 NL/h (1 NL/g/h). Once reached 330 °C, the liquid feed starts with a flowrate of 16 g/h. This means a WHSV of 2 h^{-1}, defined according to the 8 g of catalyst used.

Analogous to previous experiments of the authors, each catalyst was tested by screening with nine sets of experimental conditions, as summarised in Table 1. The used operating conditions were similar to the corresponding ones for the hydrotreating of middle distillates at the industrial scale. This methodology allowed comparison between the supported NiMoCx and CoMoCx catalysts synthesised. Changing the temperature, WHSV, and feedstock composition influenced the properties of the desulfurised gasoil and the catalyst hydrotreating effectiveness. Experimental condition sets number 1, 4, and 8 were analogous, allowing comparison of the hydrotreating effectiveness of the catalysts during the experiment under the same operating conditions and a study of its possible re-use.

Liquid products, i.e. desulfurised gasoil, were sampled every 4 h and weighed for mass balance determination. A density of 20 °C (ASTM D 4052) and refractive index of 20 °C (ASTM D 1218) were determined for each sample as a routine measurement, to identify when the steady-state had been reached. These parameters allow detecting composition changes in the liquid samples, which is mainly due to the paraffins increased occurred during co-processing. After steady-state was reached for each set of conditions, as indicated by constant values of density/refractive index with time, the liquid samples were analysed using the same analytical techniques as employed for the feedstocks. For the determination of the paraffins, the samples were dissolved in dichloromethane to a concentration of 15 mg/mL (40 vol:vol) and analysed by gas chromatography combined with mass spectrometry (GC/MS–GC system: Trace Ultra – Thermo Scientific; MS system: DSQ II – Thermo Scientific).

The reactor outlet gas was sampled at the end of the set of operating conditions using a tedlar bag. The analysis of the gaseous products was performed off-line using a GC Agilent 7890A composed of three channels: a channel HayeSep Q with a thermal conductivity detector (TCD) to measure H_2 (N_2 as the carrier gas), a channel HayeSep Q with TCD to measure O_2, N_2, CO, CO_2, SH_2, and C1-C2 hydrocarbons (He as the carrier gas), and a channel molecular sieve 5A with a flame ionisation detector to measure the C1-C7 hydrocarbons (He as carrier gas). The gas composition was characterised by Agilent's Refinery Gas analysis method.

Once each experiment completed, the used catalyst was collected, separated from SiC by sieving and washed in toluene using a Soxhlet extractor. The separation of SiC was not completely efficient, observing a residual amount of this compound in the used catalyst samples, always in the same range for all the catalysts tested. The washed catalyst samples were characterised using the same analytical methods as employed for the fresh catalyst samples.

2.3. Hydrotreating effectiveness and catalyst selectivity

The hydrotreating effectiveness of the catalysts was mainly determined based on their HDS and HDN efficiencies. These parameters can be estimated according to the following equation:

$$HDX(\%) = \frac{(X_0 - (X_p \cdot \eta))}{X_0} \cdot 100 \quad (1)$$

X= S, HDS/ X= N,HDN

where 'X_0' and 'X_P' represent the sulfur/nitrogen content of the feedstock and the liquid product, respectively (wt.%-ppm), and 'η' represents the process yield, which is defined as the quotient between the masses of organic product obtained during the reaction and the feed rate.

In the case of co-processing, it was possible to estimate the selectivity of the catalyst to the HDO or HDC/HDCn pathways, taking into account the paraffins with an even and an odd number of carbons in their chain, according to the following equations:

$$HDO\ [\%] = \frac{\Delta(\text{even paraffins})}{\Delta(\text{total paraffins [even + odd]})} \cdot 100 \quad (2)$$

$$HDC\ [\%] = \frac{\Delta(\text{odd paraffins})}{\Delta(\text{total paraffins [even + odd]})} \cdot 100 \quad (3)$$

where '*Δ(even paraffins)*' and '*Δ(odd paraffins)*' represent the paraffins resulting from triglyceride hydrotreatment that formed following the HDO (mainly nC_{14}, nC_{16}, nC_{18}, and nC_{20}) and HDC/HDCn (mainly nC_{13}, nC_{15}, nC_{17}, and nC_{19}) pathways (wt. %), respectively, and '*Δ(total paraffins [even + odd])*' represents the total paraffins formed only by the hydrotreatment of RSO (wt.%). These values are just a mathematical estimation that assumes that during co-processing there was no significant interaction between AGO and RSO.

3. Results and discussion

3.1. Catalyst characterisation

As seen from the results of the fresh catalyst characterisation (Table 2), metal impregnation occurred similarly for all the catalysts. An exception to this was observed in the case of Mo with a higher concentration in the CoMoCx samples. Moreover, the Al_2O_3-supported materials always showed higher BET surface areas (S_{BET}), which was in line with previous experiments [18] and could be related to the high activity of the catalysts. According to the elemental analysis, the carburisation was slightly more effective in the case of the CoMoCx catalysts, showing higher carbon contents. In the case of nitrogen, only a

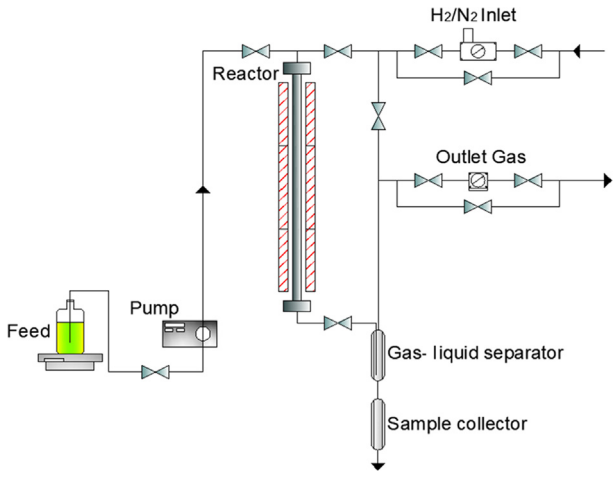

Fig. 1. Scheme of the bench-scale unit used for the hydrotreating experiments.

Table 1
Chronological description of the reaction conditions of the screening experiment.

No.	TOS (Time on stream) (h)	T (Temperature) (°C)	WHSV (h^{-1})	Feed*	Feed flowrate (g/h)
1	0–40	330	2	AGO	16
2	40–64	340	2	AGO	16
3	64–88	350	2	AGO	16
4	88–112	330	2	AGO	16
5	112–136	330	2	AGOR_5	16
6	136–160	330	2	AGOR_10	16
7	160–184	330	2	AGOR_25	16
8	184–208	330	2	AGO	16
9	208–256	330	1	AGO	8

*AGOR_X: mixtures of AGO and RSO, X = content of RSO (wt.%)

Table 2
Characterisation of the fresh catalyst samples.

Catalyst	NiMoCx/Al_2O_3	CoMoCx/Al_2O_3	NiMoCx/TiO_2	CoMoCx/TiO_2
S_{BET} (m^2/g)	146	141	76	75
Metal ICP-OES (%)	–			
Mo	13.0	15.2	12.8	15.8
Ni	2.0	–	1.9	–
Co	–	2.1	–	2.4
Al	38.0	40.7	–	–
Ti	–	–	43.7	41.8
sp*/Mo (wt.%/wt.%)	2.92	2.68	3.41	2.65
Elemental analysis (%)	–			
C	0.77	0.86	0.73	0.84
N	0.05	0.05	0.05	0.05
Mo/C ratio	0.21	0.22	0.22	0.24

* sp = support precursor metal

small amount was detected, which might mean an insignificant amount of nitride compounds in the fresh catalyst samples.

In the case of the used catalysts (Table 3), the main effect observed owing to the hydrotreating was significant carbon deposition on the catalyst surface caused by coking. This carbon deposition may be the reason for the significant reduction in S_{BET}, which could affect the hydrotreating effectiveness of the catalysts [27]. In general, the used catalyst samples showed an increase in sulfur content up to 1.32 wt%, what means partial sulfidation of the catalyst surface (residual Mo/Co/Ni oxides) during the AGO hydrotreatment. This was previously described in references [12] and does not negatively affect the catalyst activity, resulting in additional active sites for the hydrotreatment reactions. Based on previous experiments with MoCx and MoNx catalysts, metal (Mo or Ni/Co) leaching could be attributed to the mechanical attrition of the catalyst samples during their removal from the reactor.

Fig. 2 (a-d) shows the pore size distribution obtained via mercury porosimetry. The increase in carbon content owing to coking was also observed in the pore size distribution. The used catalysts were characterised by a decreased pore volume and mean pore diameter. In the case of the pore volume, the maximum decrease was observed in the Al_2O_3-supported catalysts, what was in a good agreement with the changes observed in the S_{BET} (Table 2 and Table 3), as described above. However, a higher decrease in the mean pore diameters was detected for the TiO_2-supported catalysts with an almost 24% loss compared with that of the fresh samples (from 23.4 to 24.5 to 18.4–18.7 nm). In agreement with the sulfur results from the elemental analysis of the used TiO_2-supported catalysts (1.28–1.32%), this could be explained by the partial sulfiding of molybdenum, molybdenum oxides, or the corresponding used metal promotors, suggesting the formation of sulfide compounds (MoSx, etc.) [28].

XRD analysis was performed for the fresh and used catalyst samples to characterise and identify their main crystalline phases. Fig. 3 shows the XRD diffractograms of the fresh and used catalyst samples, with the main phases detected.

According to the XRD diffractograms, all catalyst samples showed an almost amorphous carbide phase, where the peaks that correspond to the used support, Al_2O_3 (PDF 00–046-1215), or TiO_2 (PDF 00–004-0477) could be easily detected. In the same way and according to the carbon content of the fresh samples, these catalysts showed the characteristic peaks that correspond to Mo_2C (PDF 01–077-0720/04–001-2996), suggesting successful carburisation during the catalyst synthesis. The XRD diffractograms of the used catalysts were slightly different, showing the presence of MoS_2 (PDF 04–017-0898) or Co_9S_8 (PDF 00–056-0002), as a result of partial sulfidation of the catalyst surface, as previously described. Finally, the presence of the SiC phase (PDF 00–001-1118) was due to the catalyst dilution with SiC that was performed during the reactor bed loading.

3.2. Catalyst activity

Here, the reaction products and catalyst selectivity are described, followed by the influence of the operating conditions and RSO co-processing on the product properties and catalyst activities. In the same way, Co and Ni promotor effects were analysed, including the product density and HDS/HDN efficiencies, from the MoCx/Al_2O_3 and MoCx/TiO_2 catalysts [18] for the discussion of the results.

3.2.1. Reaction products and catalyst selectivity

To evaluate the products formed during the hydrotreatment reactions, it was necessary to determine the mass balance during a blank run (processing of 100 wt% AGO) and co-processing (AGO/RSO: 95/5, 90/10 and 75/25 wt%). The results of the mass balances for the NiMoCx/Al_2O_3 catalyst are shown in Table 4. The complete mass balance results are shown in Table S1 of the supplementary data.

For all experiments, the mass closure was always higher than 96% with an average value of 97.9 ± 0.6%, which suggested good mass balancing and a high reproducibility of the obtained results. The errors in the mass balances could be attributed to the use of a low-accuracy gas flow meter or liquid product losses during sampling. The increase in the reaction temperature produced an increase in the output gas and a decrease in liquid output. This effect could be caused by the slight promotion of cracking catalyst activity, as with commercial sulfide catalysts [29]. During the AGO/RSO co-processing, the added RSO was mainly converted into paraffins and CO_2, C_3H_8, and CH_4 gases. This

Table 3
Characterisation of the used catalyst samples.

Catalyst	NiMoCx/Al_2O_3	CoMoCx/Al_2O_3	NiMoCx/TiO_2	CoMoCx/TiO_2
S_{BET} (m^2/g)	105	109	57	42
Metal ICP-OES (%)	–			
Mo	8.4	9.5	8.9	9.8
Ni	1.3	–	1.0	–
Co	–	1.4	–	1.3
Al	30.4	32.6	–	–
Ti	–	–	41.9	28.3
sp*/Mo (wt.%/wt.%)	3.62	3.43	4.71	2.89
Elemental analysis (%)	–			
C	6.37	6.03	3.27	5.25
N	0.05	0.05	0.05	0.05
S	0.05	0.05	1.28	1.32
Mo/C ratio	0.02	0.02	0.03	0.02

* sp = support precursor metal

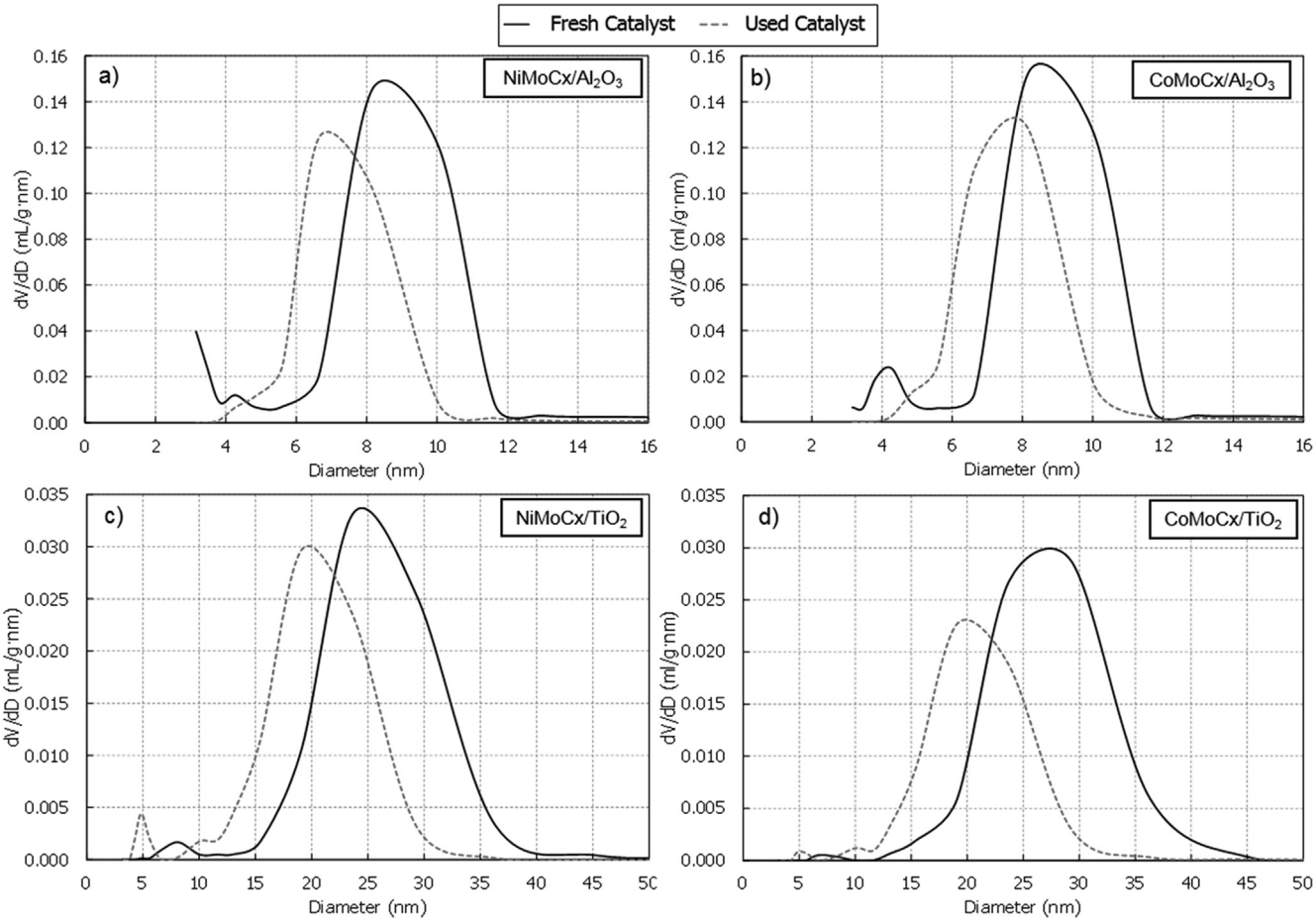

Fig. 2. Pore diameter distribution of the catalyst samples (fresh and used), as measured by mercury porosimetry.

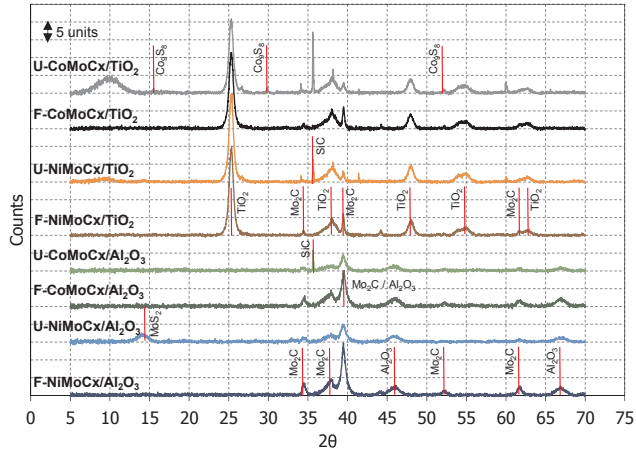

Fig. 3. XRD spectra of the fresh (F) and used (U) catalyst samples. Red lines indicates the main phases detected.

caused an increase in gas outlet, which was particularly significant at 25% RSO co-processing. In general, these results can be extended to the other mass balances shown in Table S1.

Assuming that the AGO hydrotreatment provides a similar liquid product distribution during the blank run and the co-processing, an estimation of the product yields derived from the RSO hydrotreatment was possible. Thus, the triglycerides in RSO were mainly converted to hydrogenated vegetable oil (HVO; composed of paraffins, *iso*-paraffins, and olefins) in the range of 85.2–92.7 % and to light gases in the range of 3.10–5.80 % for all the tested catalysts. Liquid water was observed as

Table 4
Mass balances during the blank run and RSO co-processing with the NiMoCx/Al_2O_3 catalyst.

NiMoCx/Al_2O_3 (%)	Feedstock input	Gas input	Liquid output	Gas output	Mass closure
Blank run	–				
330 °C-2 h^{-1}	85.1	14.9	85.1	14.9	97.7
340 °C-2 h^{-1}	85.3	14.7	85.2	14.8	98.4
350 °C-2 h^{-1}	84.9	15.1	84.6	15.4	98.6
Co-processing	–				
AGO/RSO 95/5 wt%	85.1	14.9	85.0	15.0	98.2
AGO/RSO 90/10 wt%	84.9	15.1	84.6	15.4	97.8
AGO/RSO 75/25 wt%	85.2	14.8	84.4	15.6	96.6

a by-product, especially at the AGO/RSO ratio of 75/25 wt%. However, it was not possible to extract and quantify water owing to its high dispersion in the sample vessel, which affected the accurate quantification of the organic and water phases.

To identify the main products in the desulfurised gasoil, the organic phase of the liquid products was analysed by Simdis. In the case of the blank run, a similar paraffin profile was obtained regardless of changes in the reaction temperature or WHSV. This indicated that the operating conditions did not significantly affect the composition of the desulfurised gasoil. Figure S1 in the supplementary data shows the boiling point distribution of each catalyst for the different tested operating conditions. However, this was not the case during co-processing. The paraffins from RSO deoxygenation caused a significant increase in the diesel fraction content. Fig. 4 shows the distribution of organic products from the co-processing of AGO/RSO (95/5, 90/10, and 75/25 wt%).

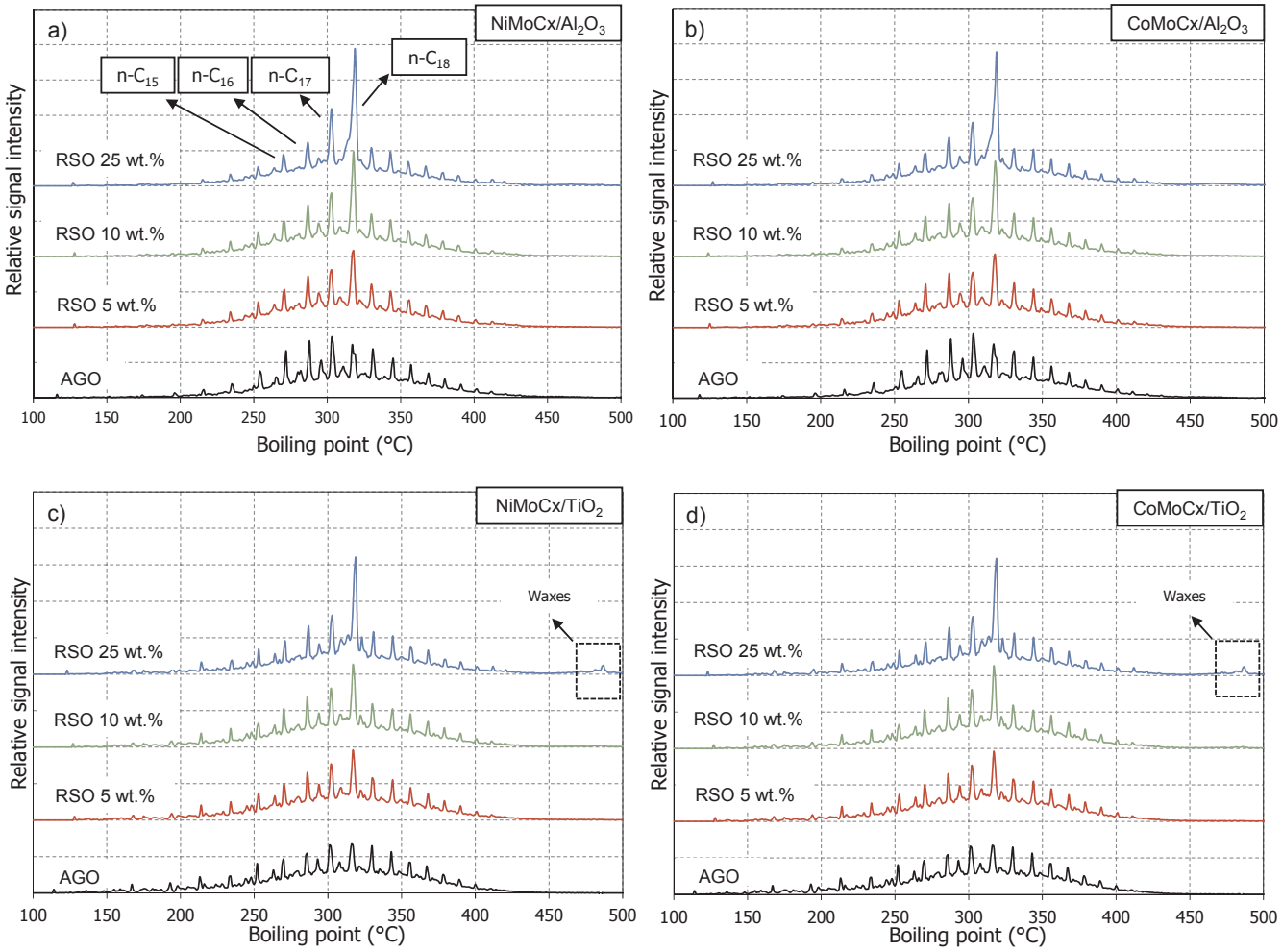

Fig. 4. Simdis results of the organic phase produced during AGO/RSO co-processing at 330 °C, 5.5 MPa and 2 h^{-1} WHSV (AGO/RSO ratios: 100/0, 95/5, 90/10 and 75/25 wt%).

As expected, the main products derived from triglyceride deoxygenation included n-C_{15} to n-C_{18} paraffins [30], which were more significant in the case of AGO/RSO at 75/25 wt%. For all the used AGO/RSO ratios and catalysts, the peak that corresponded to the n-C_{18} compound (317 °C) always showed a higher increase. This suggested that, at the operating conditions used during co-processing (330 °C, 2 h^{-1}, and 5.5 MPa), the supported NiMoCx and CoMoCx catalysts promoted the HDO pathway instead of the HDC/HDCn reactions. This catalyst selectivity might mean a higher H_2 consumption and a lower CO_x production during RSO co-processing. These results were in agreement with previous experiments of vegetable oil hydrotreating [31] or co-processing on supported MoCx and MoNx catalysts [18].

Similar to previous experiments, when TiO_2-supported catalysts were used during the co-processing of AGO/RSO at 75/25 wt% (Fig. 4 c–d), white solid particles with desulfurised gasoil were detected. These particles, considered to be 'waxes' [10], may consist of intermediate products of the deoxygenation of triglycerides to paraffins. This suggested that the TiO_2-supported catalysts were not able to carry out the complete conversion of the triglycerides to paraffins.

To quantify the catalyst selectivity for the HDO and HDC/HDCn pathways, the organic phase of the desulfurised gasoil obtained during the 75/25 wt% AGO/RSO co-processing was analysed via GC/MC. Thus, taking into account the paraffins with odd and even carbon atoms in the range of n-C_{15} to n-C_{18}, the catalyst selectivity was determined according to Equations (2) and (3). Table 5 shows the catalyst selectivity obtained for the 75/25 wt% AGO/RSO co-processing for each tested carbide catalyst.

These results correspond to the mathematical estimation. For more accurate determination, it is necessary to identify the origin of each paraffin formed due to co-processing. Due to the complexity of such a characterisation, that type of analysis was not possible to perform during these experiments. In concordance with the Simdis results, all the tested catalysts showed strong preference for the HDO pathway. This effect was significantly higher when using the TiO_2-supported catalysts and could be explained by the larger pore distribution compared with that of the Al_2O_3-supported catalysts [30]. In the case of the same support, a higher preference for the HDO pathway with Co promoted catalysts was observed.

As described in the experimental section, the output gas was sampled and analysed off-line. In general, during the blank run or the AGO/RSO co-processing, the main compound of the off-gas was H_2, and it was always in the range of 98–99 %. In the case of co-processing, this value was slightly lower due to a higher production of light gases, such as CH_4, C_3H_8, or CO_2. The distribution of gas products (calculated without H_2) during the blank run was in the following order: CH_4 in a

Table 5
Catalyst selectivity of each tested carbide catalyst.

Selectivity to:	NiMoCx/Al_2O_3	CoMoCx/Al_2O_3	NiMoCx/TiO_2	CoMoCx/TiO_2
HDO pathway (%)	66.5	69.6	73.9	78.3
HDC/HDCn pathways (%)	33.5	30.4	26.1	21.7

range of 65–75 %, C_3H_8 at 1.0–2.5%, and C_2H_6 at 0.8–1.6%. As expected, the production of these gases was dependent on the operating conditions, increasing at higher temperature or lower WHSV, similar to conventional sulfide catalysts [5]. However, the concentrations of these compounds were not significant, especially for the heavier ones. Alternatively, in the case of co-processing, the distribution of gas products changed by increasing the content of RSO in the following order: C_3H_8 (6.1–23.6%), C_3H_6 (1.2–18.3%) and CO_2 (0.5–9.5%), depending on the tested catalysts. To study the production of these light gases, it was possible to calculate them on the bases of mass balance. Fig. 5 shows the C_3H_8, C_3H_6, and CO_2 production (g/kg of processed feedstock) as a function of the RSO concentration in the feedstock at 330 °C and 2 h^{-1} WHSV. However, it was not possible to evaluate the CH_4 production or the H_2 consumption during AGO processing or AGO/RSO co-processing due to the frequent change in composition during the refinery standard gas supply (H_2: 98.5–99.5 vol% and CH_4: 0.5–1.5 vol%).

According to these results, the main effect of the vegetable oil on the gas production was a significant increase in C_3H_8, particularly when using Al_2O_3-supported catalysts. This by-product, with a high added value as biogas, increased almost linearly with the RSO content, which is plausible considering the triglyceride deoxygenation pathways [32]. Moreover, as the C_3H_8 increased, a linear increase in C_3H_6 in the off-gas was detected. In concordance with previous studies of catalytic deoxygenation of fatty acids and their derivatives [33], the presence of C_3H_6 could acts as a precursor of C_3H_8, which in the presence of H_2 will be rapidly hydrogenated to C_3H_8. However, the apparent low activity of TiO_2-supported catalysts during the co-processing was not sufficient to convert all C_3H_6 to C_3H_8, keeping it as an "intermediate" gas product. This was in line with the already described production of waxes, which was observed during the co-processing of 75/25 wt% AGO/RSO on TiO_2-supported catalysts.

The C_3H_6 production was always higher for the TiO_2-supported catalysts, regardless of the promotor used and in the same range as C_3H_8 production. In the case of the Al_2O_3-supported catalysts, both catalysts showed similar C_3H_6 production at lower ratios of AGO/RSO co-processing. However, at an AGO/RSO ratio of 75/25 wt%, CoMoCx/Al_2O_3 showed less deoxygenation activity, increasing its production or selectivity to C_3H_6, which may have indicated the higher effect of RSO addition on its hydrotreating effectiveness. This is in strong agreement with previous research on the use of Co-Mo and Ni-Mo sulfide catalysts for co-processing, suggesting that the Ni-Mo sulfide catalyst is a better choice for co-processing of vegetable oils [34,35]. Moreover, a significant increase in CO_2 during the co-processing also occurred. This side product of the HDC reaction [32] showed a higher production in the case of the TiO_2-supported catalysts, which could be justified by the lower hydrogenation activity of these catalysts. However, the lower production of CO_2 in the case of the Al_2O_3-supported catalysts could be due to the higher methanation activity of both tested catalysts, resulting in CH_4 production.

3.2.2. *Influence of the operating conditions and RSO co-processing on the product properties*

As previously mentioned, changing the operating conditions and the addition of RSO to the feedstock resulted in significant changes in the product properties, mainly in the density and bromine index. Table 6 shows the characterisation of AGO and RSO used during the co-

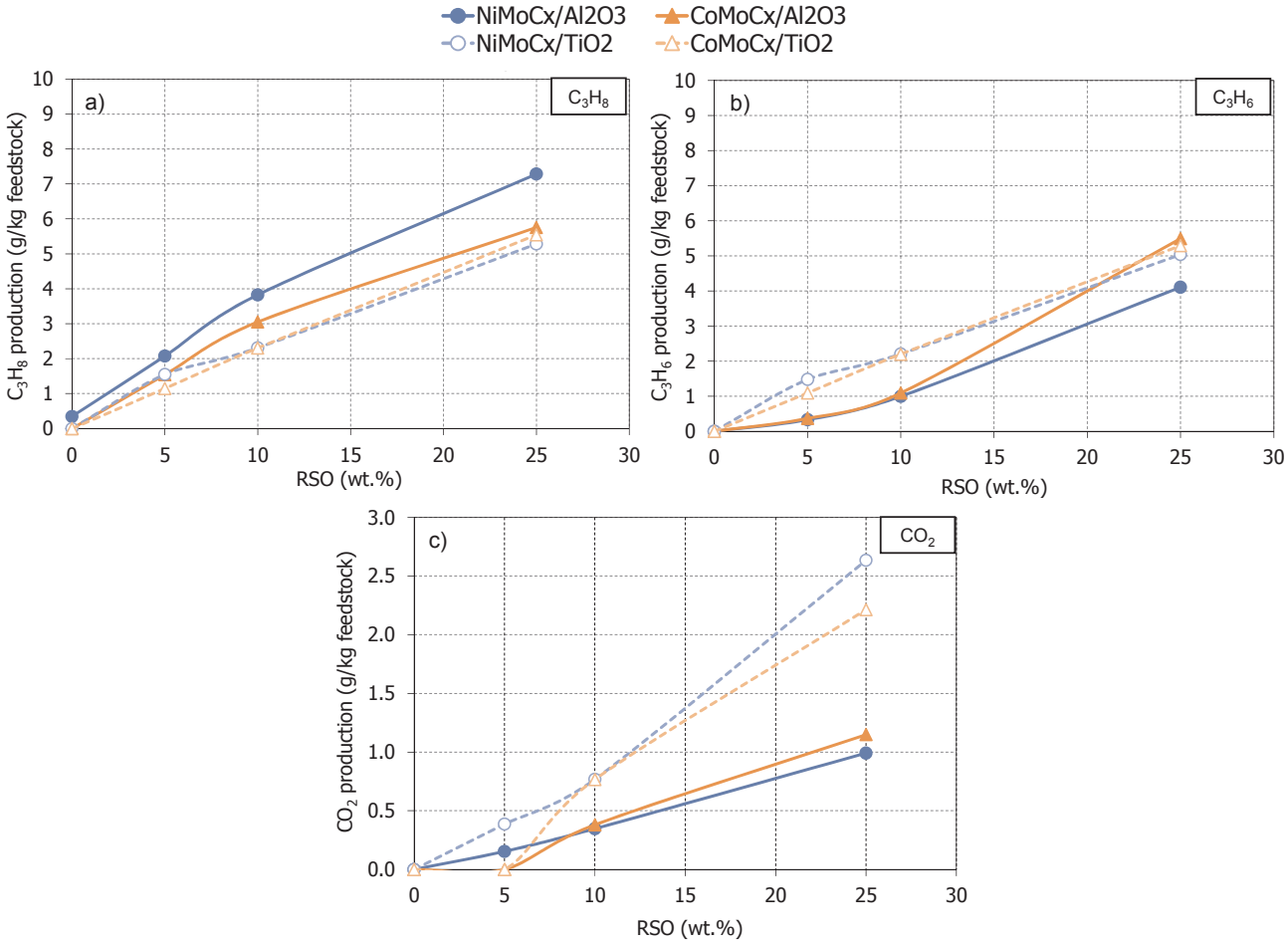

Fig. 5. Light gas production per kg of feedstock during AGO/RSO co-processing at 330 °C, 5.5 MPa and 2 h^{-1} WHSV. Results at 0 wt% RSO corresponds to 100 wt% AGO hydrotreatment.

Table 6
Basic feedstock properties.

Property	AGO	RSO	Standard test method
Density at 20 °C (kg/m^3)	853.6	914.4	ASTM D 4052
Refractive index at 20 °C	1.4763	1.4723	ASTM D 1218
S content (wt.%.-ppm)	1.10 wt%	2.50 ppm	ASTM D 1552
N content (ppm)	239	1.60	ASTM D 5291
Acid number (mg KOH/g)	0.04	0.20	ASTM D 664
Bromine index (mg Br/g)	8211	30,460	ASTM D 1492
Elemental analysis (%)	–		ISO 29,541
C content	86.4	75.5	
H content	13.5	11.7	
Simdis (wt.%)	–		ASTM D 2887
10	221	597	
30	280	606	
50	309	609	
70	336	612	
90	374	613	

processing.

As expected, both feedstocks showed the common characteristics of a middle distillate or vegetable oil, respectively. During hydrotreating, the density of the products changes. Fig. 6 shows the effect of the operating conditions on the density at 20 °C. Fig. 6 c–d shows the product densities from Mo, Co-Mo, and Ni-Mo carbide catalysts in relative terms.

By analogy to conventional sulfide catalysts, a significant increase in the reaction temperature contributed to a decrease in the product density [27]. This may mean an increase in hydrogenation/hydrocracking activity. A similar behaviour was detected with a decrease in WHSV. For all the tested operating conditions, the Al_2O_3-supported catalysts always produced desulfurised gasoil with a lower density. This behaviour was also shown in comparison with that of monometallic catalysts (Fig. 7 c–d). As shown by the results, the addition of Ni or Co as a promotor resulted in a product with a lower density, indicating an increase in the hydrogenation/hydrocracking activity of the catalysts. However, an exception to this behaviour was found for CoMoCx/TiO_2, which produced a desulfurised gasoil with a higher density. This could be related to the lower hydrogenation activity of this catalyst, despite the Co promotor effect.

In the case of co-processing, the influence over the density decrease was highlighted. This effect was due to the lower densities of the paraffins that proceeded from RSO deoxygenation compared with those of common gasoil compounds [36]. Fig. 7 shows the effect of vegetable oil addition on the density at 20 °C for the supported Mo, Co-Mo, and Ni-Mo carbide catalysts.

In general, for all the tested catalysts, the product density decreased linearly with an increase in the RSO content. Thus, the Al_2O_3-supported catalysts resulted in the products with the lower density. This could mean a higher hydrogenation/hydrocracking activity for these catalysts during co-processing. However, at high ratios of RSO, the CoMoCx/Al_2O_3 catalyst produced a desulfurised gasoil with a higher density than expected, taking into account the results provided by the NiMoCx/Al_2O_3 catalyst. This behaviour, which is in line with the increase in C_3H_6 detected for the AGO/RSO co-processing at 75/25 wt% (Fig. 5),

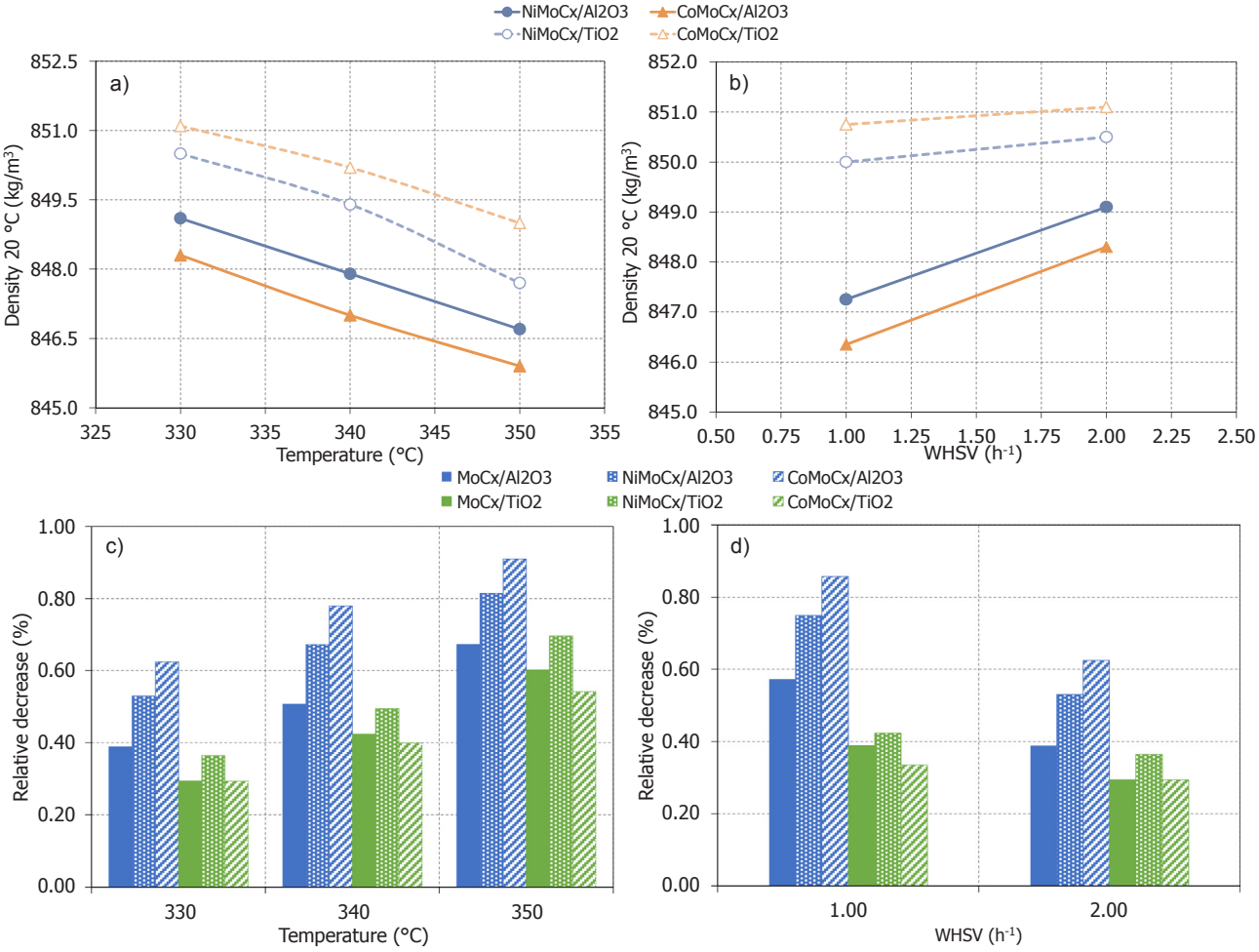

Fig. 6. Densities measured at 20 °C for the hydrotreating of 100 wt% AGO at different operating temperatures (a) and WHSVs (b) and the comparison of product densities from Mo, Co-Mo and Ni-Mo carbide catalysts at different temperatures (c) and WHSVs (d).

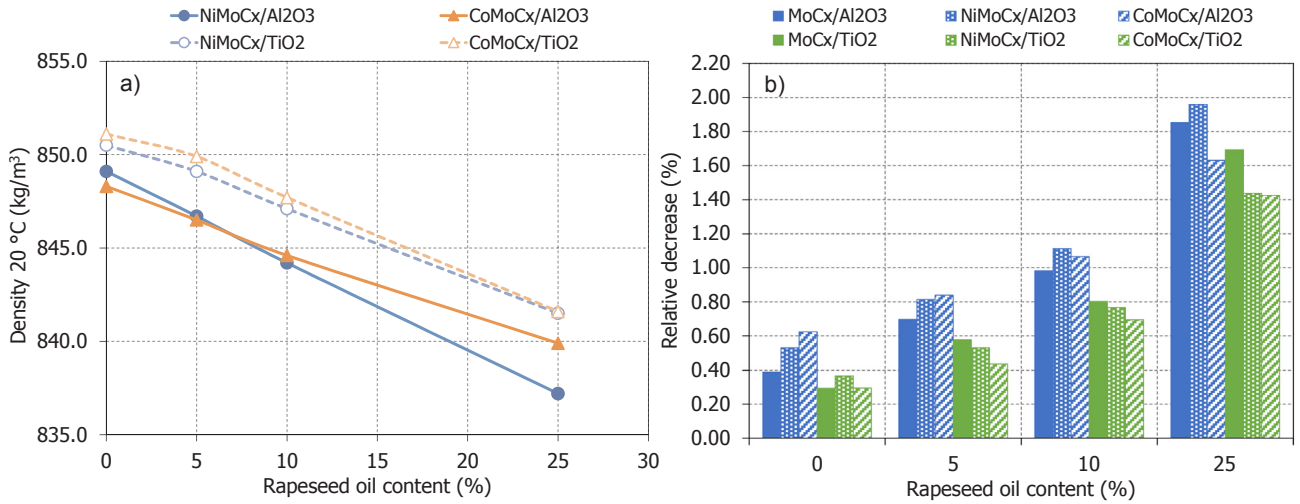

Fig. 7. Densities measured at 20 °C for the co-processing of different AGO/RSO mixtures at 330 °C, 5.5 MPa and 2 h^{-1} WHSV (a) and comparison of product densities from Mo, Co-Mo and Ni-Mo carbide catalysts at the same operating conditions (b). Results at 0 wt% RSO corresponds to 100 wt% AGO hydrotreatment.

may mean a decrease in the hydrogenation efficiency for the CoMoCx/Al_2O_3 catalyst at higher AGO/RSO ratios. Moreover, upon comparing the product densities for the mono- and bi-metallic catalysts, a higher influence of co-processing in the promoted catalysts was detected, resulting in products that had a higher density. An exception to this behaviour was the NiMoCx/Al_2O_3 catalyst, which always produced the product with the lowest density.

While no significant changes were observed in the elemental analysis or acid number of the desulfurised gasoil due to the RSO co-processing, this was not the case for the bromine index. This parameter, which is related to the saturation of double bonds, indicated changes in the hydrogenation efficiency of the carbide catalysts owing to the influence of the operating conditions or RSO co-processing. Fig. 8 shows the bromine index of the desulfurised gasoil under different operating conditions.

When the reaction temperature increased, each catalyst showed a different behaviour owing to its support or promotor metal. In this way, the NiMoCx/Al_2O_3 catalyst showed a decreasing trend with an increase in the temperature, which is in accordance with the conventional catalysts used for hydrotreatment [37]. In contrast, CoMoCx/Al_2O_3 showed an initial decrease in the bromine index at 340 °C followed by an increase at 350 °C, similar to the TiO_2-supported catalysts. This discrepancy in the expected behaviour may mean a decrease in the hydrogenation efficiency at that particular reaction temperature, increasing the content of unsaturated compounds in the organic liquid product. Additionally, a decrease in the WHSV resulted in an increase in the bromine index. This was opposite to what was expected and could be induced by the deterioration of the hydrogenation efficiency of the catalysts at the end of the experiment. Thus, the carbon deposits detected in the used catalysts (Table 3) hardly affected the S_{BET} and the porous structure of the catalysts, blocking the active sites and decreasing their activity.

Analogous to the operating conditions, the addition of RSO also affected the saturation of the desulfurised gasoil. Fig. 9 shows the dependence of the RSO content on the bromine index during the AGO/RSO co-processing.

The addition of RSO affected the hydrogenation efficiency more significantly than in the case of the operating conditions. Thus, an increase in the bromine index with RSO content was observed. An exception to this behaviour was observed with the NiMoCx/Al_2O_3 catalyst, which at lower AGO/RSO ratios showed a decrease in the bromine index. In agreement with the density results, this may indicate better stability of this catalyst during co-processing, maintaining the hydrogenation efficiency during AGO processing.

3.2.3. Influence of the operating conditions and RSO co-processing on the HDS/HDN efficiencies

The addition of RSO increased the presence of heteroatoms in the

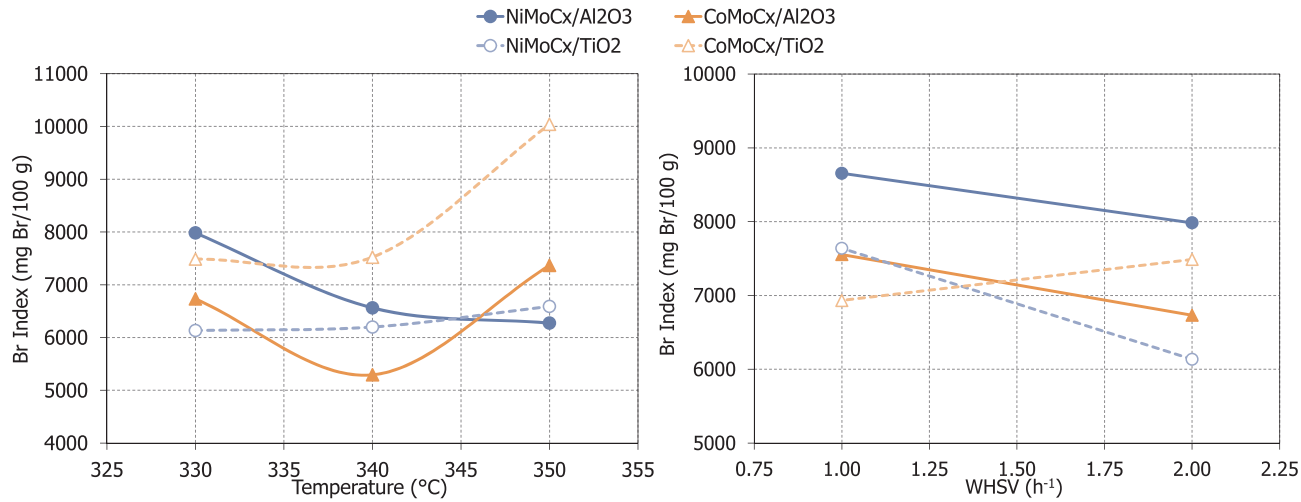

Fig. 8. Bromine indices measured for the hydrotreating of 100 wt% AGO at different operating temperatures (a) and WHSVs (b).

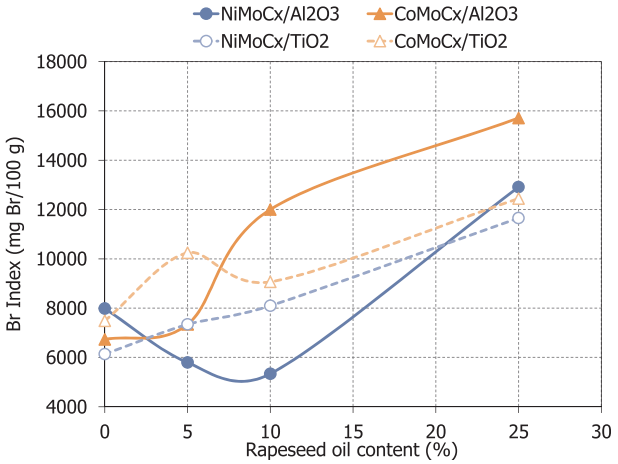

Fig. 9. Bromine indices measured for the co-processing of different AGO/RSO mixtures at 330 °C, 5.5 MPa and 2 h^{-1} WHSV. Result at 0 wt% RSO corresponds to 100 wt% AGO hydrotreatment.

feedstock. This could significantly affect the HDS and HDN efficiencies of the catalysts (Equation (1)). As described above, first, the influence of the operating conditions during the AGO processing are described; then, the effect of RSO addition was analysed. Fig. 10 shows the HDS and HDN efficiencies during the blank run under different operating conditions.

As expected, an increase in the operating temperature (from 330 to 350 °C) caused a significant improvement in the HDS/HDN efficiencies [38]. In concordance with previous results [18], the Al_2O_3-supported catalysts showed the highest HDS efficiency. This was particularly significant in the case of the CoMoCx/Al_2O_3 catalyst with a HDS efficiency up to 80%. In the case of HDN efficiency, the observed behaviour was slightly different. Thus, while CoMoCx/Al_2O_3 again showed the highest efficiency, the TiO_2-supported catalysts showed a higher HDN efficiency than NiMoCx/Al_2O_3. A similar behaviour was observed in the case of changing the WHSV. Thus, the catalysts always showed higher HDS/HDN efficiencies at lower WHSV. This was particularly significant in the case of the NiMoCx/Al_2O_3 catalyst with a HDS efficiency increase up to 30%.

Upon comparing the HDS/HDN efficiencies of mono- and bi-metallic catalysts, it is possible to claim that Co and Ni addition significantly improves the HDS efficiency [12,23]. However, this was not the case for the HDN efficiency, and we observed higher values in the case of MoCx catalysts at higher operating temperatures or lower WHSV.

In the case of co-processing, the behaviour of each catalyst was different owing to the amount of RSO added into the feedstock. Fig. 11 shows the effect of RSO co-processing on the HDS and HDN efficiencies.

As in the blank run, the bimetallic Al_2O_3-supported catalysts always showed a higher HDS efficiency than the TiO_2-supported catalysts. Specifically, the CoMoCx/Al_2O_3 catalyst again showed higher values for RSO co-processing rates up to 10 wt%. However, at higher rates, its HDS efficiency decreased in accordance with the product properties and gas results previously described, which indicated a decrease in the

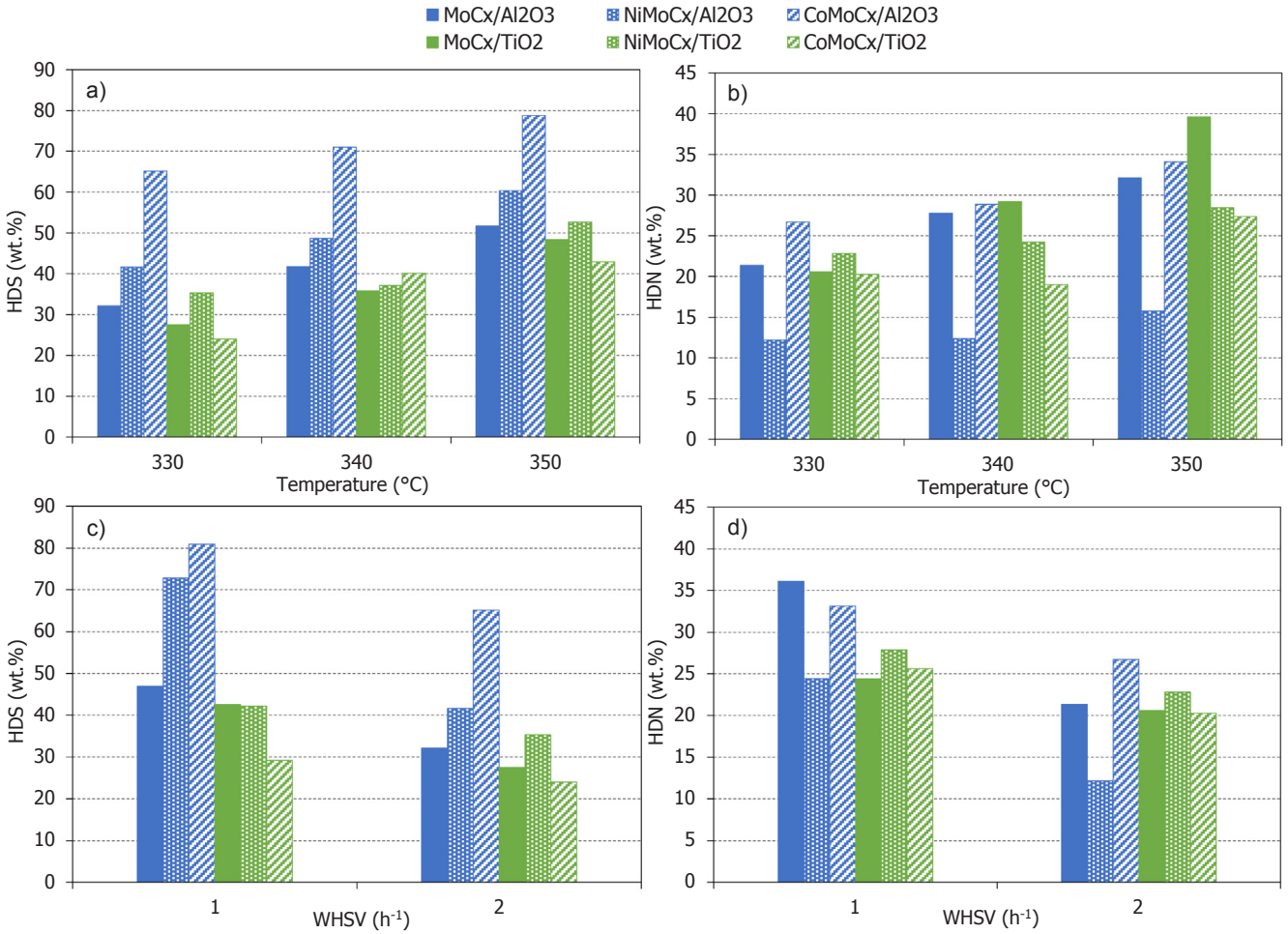

Fig. 10. HDS and HDN efficiencies of Mo, Ni-Mo and Co-Mo carbide catalyst during the hydrotreatment of 100 wt% AGO at different operating temperatures (a and b) and WHSVs (c and d).

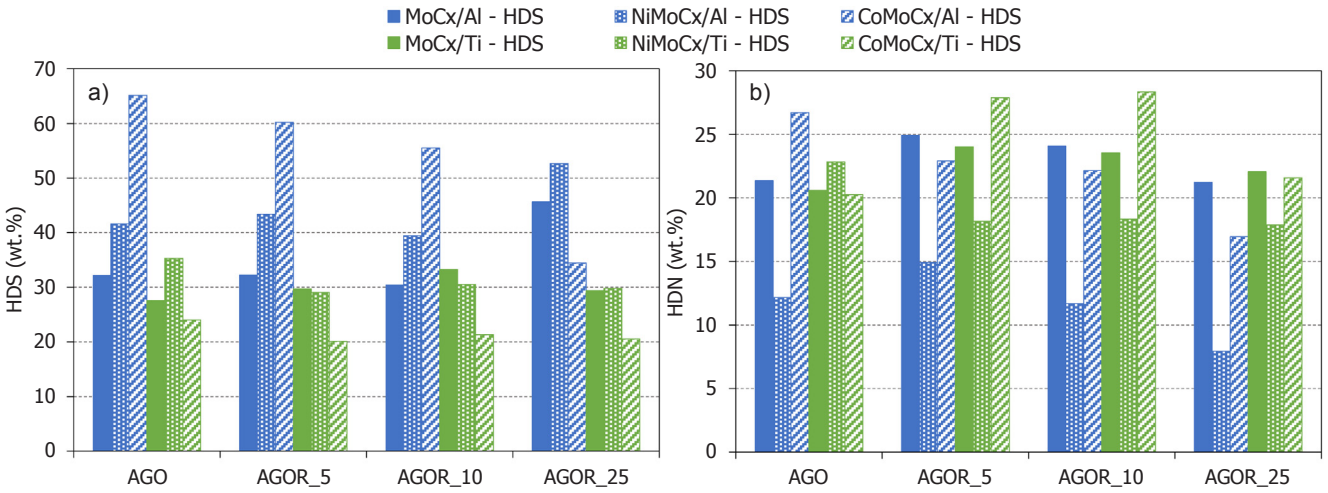

Fig. 11. HDS (a) and HDN (b) efficiencies of Mo, Ni-Mo and Co-Mo carbide catalysts for the co-processing of different AGO/RSO mixtures at 330 °C, 5.5 MPa and 2 h^{-1} WHSV (AGO/RSO ratios: 100/0, 95/5, 90/10 and 75/25 wt%).

hydrogenation effectiveness. This could be due to the competition between the HDS/HDN reactions and the deoxygenation of triglycerides [34], which occurs mainly at the AGO/RSO ratio of 75/25 wt%. However, the behaviour of the NiMoCx/Al_2O_3 catalyst was different, showing better HDS efficiency at higher ratios of RSO (up to 55% of the HDS efficiency), suggesting a lower influence of the co-processing on its hydrotreating effectiveness for sulfur removal. This observed effect could be related to an inhibition of Co-Mo catalysts activity due to the effect of side products derived from the deoxygenation (CO, CO_2, and H_2O), analogous to the effect observed in the conventional CoMo/Al_2O_3 sulfide catalysts during the co-processing of vegetable oils [39]. Moreover, the TiO_2-supported catalysts, despite exhibiting lower HDS efficiencies, were less affected by RSO addition, exhibiting approximately the same HDS efficiency during co-processing.

In the case of the HDN reactions, the observed behaviour was different. Thus, while NiMoCx/TiO_2 and the Al_2O_3-supported catalysts showed a decrease in the HDN efficiency during co-processing, the CoMoCx/TiO_2 did not, showing a slight increase in the hydrotreating effectiveness for nitrogen removal. Upon analysing the HDS/HDN efficiencies for the mono- and bi-metallic catalysts during co-processing, we can claim that the Ni- or Co-promoted catalysts were more affected by RSO addition, particularly in terms of the HDN efficiency.

As described in the Experimental section (Table 1), experimental sets number 1 (330/1), 4 (330/2), and 8 (330/3) were performed under the same operating conditions, i.e. 330 °C, 5.5 MPa, and 2 h^{-1}. This was done to compare the most noteworthy changes in the hydrotreating effectiveness of the catalysts. Fig. 12 shows the HDS/HDN efficiencies of the catalyst samples for the experimental condition sets of 1, 4, and 8.

According to the results, despite the coking observed on the catalyst surface, the HDS/HDN efficiencies did not show a significant decrease. This could be due to the partial sulfidation detected in the used catalysts [12] (Table 3), what could balance the loss of activity owing to the carbon deposit. Thus, after thermal treatment to eliminate the deposited coke on the catalyst surface, there could be plausible re-use of the catalysts in a second experiment.

4. Conclusions

Four sulfur-free-supported (Al_2O_3 and TiO_2) Ni-Mo and Co-Mo carbide catalysts were synthesised and tested during the hydrotreating of atmospheric gasoil (AGO) and during its co-processing with rapeseed oil (RSO) as possible alternatives to conventional sulfide hydrotreatment catalysts. An increase in the operating temperature (from 330 to 350 °C) and a decrease in the feeding rate (from 2 to 1 h^{-1}) led to a significant improvement in the product properties (density and brome index) and the hydrotreating effectiveness, which were particularly significant for the CoMoCx/Al_2O_3 catalysts, with a hydrodesulfurisation

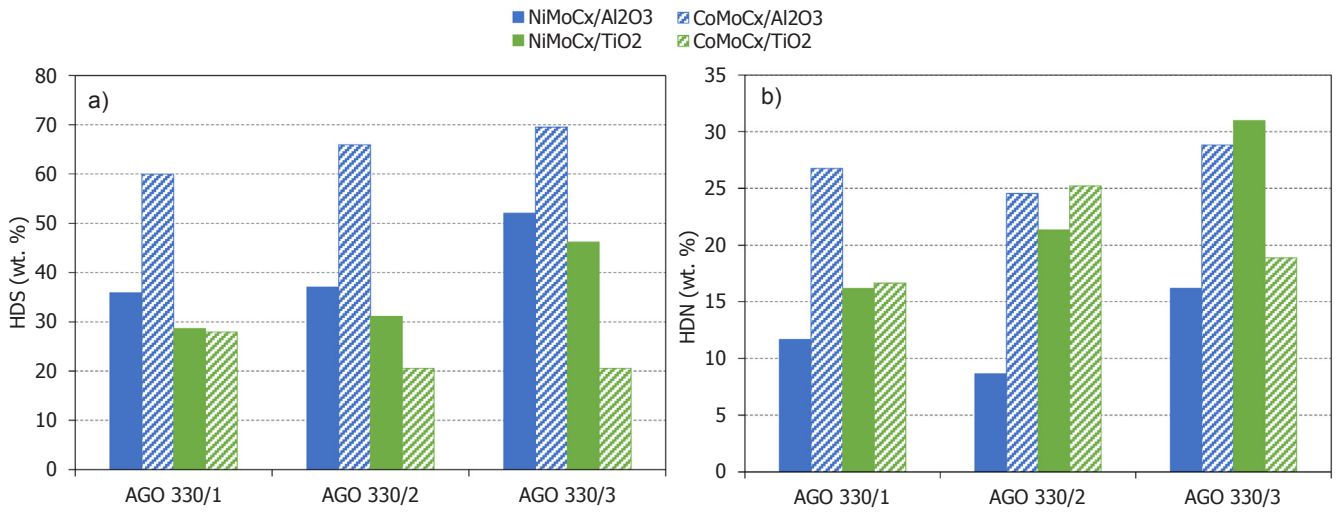

Fig. 12. HDS (a) and HDN (b) efficiencies of Ni-Mo and Co-Mo carbide catalysts at 330 °C, 5.5 MPa and 2 h^{-1} WHSV at different TOS of experiment.

efficiency of up to 80% at 350 °C. For co-processing, all the catalysts mainly promoted the hydrodeoxygenation pathway (65–72%) to the detriment of the (hydro)decarboxylation/decarbonylation reactions (22–34%) during the triglyceride deoxygenation (AGO/RSO of 75/25 wt%), which meant a strong selectivity of the NiMoCx and CoMoCx catalysts towards C–O/C = O cleavage instead of towards C–C scission. Based on the Simdis results, the Al_2O_3-supported carbide catalysts completely converted the triglycerides into paraffins, resulting in a significant decrease in the product density at higher RSO ratios in the feedstock. In terms of hydrotreating effectiveness, the $CoMoCx/Al_2O_3$ and $NiMoCx/Al_2O_3$ catalysts were found to be the most efficient for hydrodesulfurisation at lower (AGO/RSO of 90–95/5–10 wt%) and higher (AGO/RSO of 75/25 wt%) ratios of RSO. Therefore, our results have shown that improving the catalytic properties of sulfur-free alumina supported Mo Carbides with Ni/Co promoters, make them promising alternatives to conventional catalysts for the hydrotreatment of the middle distillates with vegetable oils.

CRediT authorship contribution statement

Héctor De Paz Carmona: Conceptualization, Validation, Formal analysis, Investigation, Data curation, Writing - original draft, Writing - review & editing, Visualization, Project administration. **Uliana Akhmetzyanova:** Conceptualization, Investigation, Data curation, Writing - review & editing, Visualization. **Zdeněk Tišler:** Conceptualization, Resources, Writing - review & editing, Supervision. **Pavla Vondrová:** Resources, Visualization, Writing - review & editing.

Declaration of Competing Interest

The authors declare that they have no known competing financial interests or personal relationships that could have appeared to influence the work reported in this paper.

Acknowledgements

This work is a result of the Development Project of UniCRE (project code LO1606), which was financially supported by the Ministry of Education, Youth and Sports of the Czech Republic (MEYS) through National Sustainability Programme I.

The results were obtained by using the infrastructure of the project Efficient Use of Energy Resources Using Catalytic Processes (LM2015039), which was financially supported by MEYS within the broader scope of large infrastructures.

Appendix A. Supplementary data

Supplementary data to this article can be found online at https://doi.org/10.1016/j.fuel.2020.117363.

References

[1] Bezergianni S, Dimitriadis A. Comparison between different types of renewable diesel. Renew Sust Energ Rev. 2013;21:110–6.
[2] Hájek M, Skopal F, Kwiecien J. Biodiesel preparation in a batch emulsification reactor. Eur. J. Lipid. Sci. Technol. 2009;111:979–84.
[3] De Paz Carmona H, Horáček J, Brito Alayón A, Macías Hernández JJ. Suitability of used frying oil for co-processing with atmospheric gas oil. Fuel 2018;214:165–73.
[4] De Paz Carmona H, Romero Vázquez MA, Frontela Delgado J, Macías Hernández JJ, Brito Alayón A. Catalytic co-processing of used cooking oil with straight run gas oil in a hydrotreatment pilot plant. Hydrocarb. Process. 2016;95:59–66.
[5] Schuit GCA, Gates BC. Chemistry and Engineering of catalytic Hydrodesulfurization. AICHE J. 1973;3(19):417–38.
[6] Kim SK, Han JY, Lee H, Yum T, Kim Y, Kim J. Production of renewable diesel via catalytic deoxygenation of natural triglycerides: Comprehensive understanding of reaction intermediates and hydrocarbons. Appl. Energ. 2014;116:199–205.
[7] Jęczmionek L, Porzycka-Semczuk K. Hydrodeoxygenation, decarboxylation and decarbonylation reactions while co-processing vegetable oils over a NiMo hydrotreatment catalyst. Part I: Thermal effects – Theoretical considerations. Fuel 2014;131:1–5.
[8] Donnis B, Egeber RG, Blom P, Knudsen KG. Hydroprocessing of bio-oils and oxygenates to hydrocarbons. Understanding the reactions routes. Top Catal 2009;52:229–40.
[9] Bezergianni S, Dimistriadis A, Kikhtyanin O, Kubička D. Refinery co-processing of renewable feeds. Prog energy combust 2018;68:29–64.
[10] Kubička D, Horáček J. Deactivation of HDS catalysts in deoxygenation of vegetable oils. Appl. Catal. A-Gen. 2011;394:9–17.
[11] Bezergianni S, Dimitriadis A, Karonis D. Diesel decarbonization via effective catalytic Co-hydroprocessing of residual lipids with gas-oil. Fuel 2014;136:366–73.
[12] Furimsky E. Metal carbides and nitrides as potential catalysts for hydroprocessing. Appl. Catal. A-Gen. 2003;240:1–28.
[13] Da Costa P, Potvin C, Manoli JM, Genin B, Djéga-Mariadassou G. Deep hydrodesulphurization and hydrogenation of diesel fuels on alumina-supported and bulk molybdenum carbide catalysts. Fuel 2004;83:1717–26.
[14] Da Costa P, Manoli JM, Potvin C, Djéga-Mariadassou G. Deep HDS on doped molybdenum carbides: From probe molecules to real feedstocks. Catal. Today 2005;107–108:520–30.
[15] Sousa LA, Zotin JL, Da Silva VT. Hydrotreatment of sunflower oil using supported molybdenum carbide. Appl. Catal. A: Gen. 2012;449:105–11.
[16] Wang H, Yan S, Salley SO, Simon Ng KY. Support effects on hydrotreating of soybean oil over NiMo carbide catalyst. Fuel 2013;111:81–7.
[17] Dhandapani B, Clair TSt, Oyama ST.. Simultaneous hydrodesulfurization, hydrodeoxygenation and hydrogenation with molybdenum carbide. Appl Catal A-Gen 1998;168:219–28.
[18] De Paz Carmona H, Horáček J, Tišler Z, Aktmetzyanova U. Sulfur free supported MoCx and MoNx Catalysts for the hydrotreatment of Atmospheric gasoil and its blends with rapeseed oil. Fuel 2019;254:115582.
[19] Huber GW, O'Connor P, Corma A. Processing biomass in conventional oil refineries: Production of high quality diesel by hydrotreating vegetable oils in heavy vacuum oil mixtures. Appl Catal A-Gen 2007;329:120–9.
[20] De Paz Carmona H, de la Torre Alfaro O, Brito Alayón A, Romero Vázquez MA, Macías Hernández JJ. Co-processing of straight run gas oil with used cooking oil and animal fats. Fuel 2019;254:115583.
[21] Arun N, Sharma RV, Dalai AK. Green diesel synthesis by hydrodeoxygenation of bio-base feedstocks: Strategies for catalyst design and development. Renew. Sust. Energ. Rev. 2015;48:240–55.
[22] Trimm DL. Design of industrial catalysts. The Netherlands: Elsevier Scientific Publishing Company; 1980.
[23] Diaz B, Sawhill SJ, Bale DH, Main R, Phillips DC, Korlann S, et al. Hydrodesulfurization over supported monometallic, bimetallic and promoted carbide and nitride catalysts. Catal. Today 2003;86:191–209.
[24] Guangzhou J, Jianhua Z, Xiuju F, Guida S, Junbin G. Effect of Ni promoter on Dibenzothiophene Hydrodesulfurization Performance of Molydenum carbide catalyst. Chinese J. Catal 2006;27(10):899–903.
[25] Tišler Z, Velvarská R, Skuhrovcová L, Pelíšková L, Akhmetzyanova U. Key Role of Precursor Nature in Phase Composition of Supported Molybdenum Carbide and Nitrides. Materials 2019;12:415.
[26] Afanasiev P. New Single Source Route to the Molybdenum Nitride Mo_2N. Inor. Chem. 2002;41(21):5317–9.
[27] Li X, Luo X, Jin Y, Li J, Zhang H, Zhang A, et al. Heterogeneous sulfur-free hydrodeoxygenation catalysts for selectively upgrading the renewable bio-oils to second generation biofuels. Renew. Sust. Energ. Rev. 2018;82:3762–97.
[28] Prasada Rao TSR, Murali Dhar G. Recent Advances in Basic and Applied Aspects of Industrial Catalysis. Dehradum, India: Elsevier; 1998.
[29] Wang F, Xu J, Jiang J, Liu P, Li F, Ye J, et al. Hydrotreatment of vegetable oil for green diesel over activated carbon supported molybdenum carbide catalyt. Fuel 2018;216:738–46.
[30] Wang H, Yan S, Salley SO, Simon KY. Support effects on hydrotreating of soybean oil over NiMo carbide catalyst. Fuel 2013;111:81–7.
[31] Ren H, Yu W, Salciccioli M, Chen Y, Huang Y, Xiong K, et al. Selective hydrodeoxygenation of biomass-derived oxygenates to unsaturated hydrocarbons using molybdenum carbide catalysts. ChemSusChem 2013;6:798–801.
[32] Gosselink RW, Hollak SAW, Chang SW, Haveren J, Jong K, Bitter JH, et al. Reaction Pathways for the Deoxygenation of Vegetable Oils and Related Model Compounds. ChemSusChem 2013;6:1576–94.
[33] Mäki-Arvela P, Kubickova I, Snåre M, Eränen K, Murzin DY. Catalytic Deoxygenation of Fatty Acids and Their Derivatives. Energy Fuels 2007;21:30–41.
[34] Bezegianni S, Dimitriadis A, Meletidis G. Effectiveness of CoMo and NiMo catalysts on co-hydroprocessing of heavy atmospheric gas oil-waste cooking oil mixtures. Fuel 2014;125:129–36.
[35] Egeberg R, Michaelsen N, Skyum L, Zeuthen P. Hydrotreating in the production of green diesel. PTQ 2010;Q2.
[36] Walendziewski J, Stolarski M, Łużny R, Klimek B. Hydroprocessing of light gas oil – rape oil mixtures. Fuel Process. Technol. 2009;90:686–91.
[37] Bezegianni S, Dimitriadis A. Temperature effect of co-hydroprocessing of heavy gas oil-waste cooking oil mixtures for hybrid diesel production. Fuel 2013;103:579–84.
[38] Mochida I, Choi KH. An Overview of Hydrodesulfurization and Hydrodenitrogenation. J. Jpn. Petrol. Inst. 2004;47(3):145–63.
[39] Al-Sabawi M, Chen J. Hydroprocessing of Biomass-Derived Oils and Their Blends with Petroleum Feedstocks: A Review. Energ. Fuel 2012;26:5373–99.